

Exchange interaction and its tuning in magnetic binary chalcogenides

M. G. Vergniory,^{1,*} D. Thonig,¹ M. Hoffmann,^{1,2} I. V. Maznichenko,² M. Geilhufe,¹ M. M. Otrokov,³ X. Zubizarreta,^{1,4} S. Ostanin,¹ A. Marmodoro,¹ J. Henk,² W. Hergert,² I. Mertig,^{1,2} E. V. Chulkov,^{3,4,5} and A. Ernst^{1,†}

¹Max-Planck-Institut für Mikrostrukturphysik, Weinberg 2, 06120 Halle, Germany

²Institut für Physik, Martin-Luther-Universität Halle-Wittenberg, D-06099 Halle, Germany

³Physics Department, Tomsk State University, pr. Lenina 36, 634050 Tomsk, Russia

⁴Donostia International Physics Center, P. de Manuel Lardizabal 4, San Sebastián, 20018 Basque Country, Spain

⁵Departamento de Física de Materiales, Facultad de Ciencias Químicas, Apdo. 1072, San Sebastián, 20080 Basque Country, Spain

(Dated: August 13, 2018)

Using a first-principles Green's function approach we study magnetic properties of the magnetic binary chalcogenides Bi_2Te_3 , Bi_2Se_3 , and Sb_2Te_3 . The magnetic coupling between transition-metal impurities is long-range, extends beyond a quintuple layer, and decreases with increasing number of d electrons per $3d$ atom. We find two main mechanisms for the magnetic interaction in these materials: the indirect exchange interaction mediated by free carriers and the indirect interaction between magnetic moments via chalcogen atoms. The calculated Curie temperatures of these systems are in good agreement with available experimental data. Our results provide deep insight into magnetic interactions in magnetic binary chalcogenides and open a way to design new materials for promising applications.

PACS numbers: 71.70.Ej, 72.15.Jf, 85.80.Fi

Tetradymite chalcogenides, in particular Bi_2Te_3 , Bi_2Se_3 , and Sb_2Te_3 , are of great interest due to their outstanding structural and electronic properties. These compounds consist of repeated blocks of five atomic layers (quintuple layers) separated by a van der Waals gap. The electronic structure features a narrow band gap and strong spin-orbit coupling, which are responsible for the inverted band structure at the Brillouin zone center Γ . Tetradymite chalcogenides are attractive for thermoelectric applications [1] because of their high figure of merit at room temperature. Recently, topologically protected surface states have been observed in all of these chalcogenides, which makes them subject of intense research [2, 3]. Especially, these bichalcogenides serve as a basis for new materials with desired properties [4]. This is feasible by stacking of different compounds or specific doping. In particular, doping with magnetic impurities can open new perspectives for spintronics and spin caloritronics applications [5–8].

The aim of this work is to study the magnetic properties of tetradymite chalcogenides doped with transition metal impurities. Some of these systems were already studied as possible candidates for spintronics applications some years ago [9–19]. Most of the experiments were done on single crystals with a maximal doping concentration of $x = 0.1$. Thereby, stable ferromagnetic order was observed mostly in chalcogenides doped with vanadium and chromium [9, 11, 13], while samples doped with manganese were found either ferromagnetic at very low temperatures or antiferro- and paramagnetic depending on experimental conditions and sample preparation [10, 12, 17–19]. High Curie temperatures were reported

for films prepared with molecular-beam epitaxy: 177 K and 190 K for $\text{Sb}_{1.65}\text{V}_{0.35}\text{Te}_3$ and $\text{Sb}_{1.41}\text{Cr}_{0.59}\text{Te}_3$, respectively [15, 16]. The great interest in breaking of time reversal symmetry in topological insulators motivated further investigations of magnetic impurities located in particular at the surfaces of tetradymite chalcogenides [19–26].

Magnetic properties of magnetic chalcogenides can be efficiently described by first-principles methods. One of the first comprehensive studies was carried out by Larson and Lambrecht [27], who investigated the electronic and magnetic properties of bulk Bi_2Te_3 , Bi_2Se_3 , and Sb_2Te_3 doped with $3d$ transition metal atoms; their results for magnetically doped Bi_2Se_3 were confirmed by several groups [28, 29]. Recently, it was shown that the Dirac surface state of the topological insulator Bi_2Te_3 survives upon moderate Mn doping of the surface layer, but can lose its topological nontrivial character depending on the magnetization direction [30, 31]. However, critical magnetic properties and the exchange interaction in magnetic chalcogenides were not studied in detail on a theoretical *ab initio* level and, thus, are still under debate.

In this work, doping bulk tetradymite chalcogenides with transition metals by means of a first-principles Green's function method, we show that the exchange interaction in these materials can be either long-range ferromagnetic, antiferromagnetic or paramagnetic, depending on the host and the impurity atoms. We identify in particular two main types of magnetic interactions and discuss ways to manipulate the magnetic properties of these systems.

The calculations were performed within the density

functional theory using the local spin density approximation (LSDA) and the generalized gradient approximation (GGA) [32, 33]. A self-consistent Green's function method in both relativistic and scalar-relativistic implementations was used to compute electronic and magnetic properties of the magnetic chalcogenides. Substitutional disorder was treated within the coherent potential approximation (CPA; e.g. [34]). Heisenberg exchange constants J_{ij} were obtained using the magnetic force theorem as it is implemented within the multiple-scattering theory [35]. Inclusion of spin-orbit coupling leads to minor changes in the magnetic interaction (about 3-5% with respect to the scalar-relativistic case). Therefore, for the sake of clarity, here we present only exchange constants calculated within the scalar-relativistic approximation.

According to the available experimental data [9–20, 24, 25], 3d transition metal impurities in bulk tetradymite chalcogenides substitute typically cation atoms (Bi and Sb) and can supply 1–3 electrons for the bonding. The comparably smaller size of transition metal ions may lead to substantial relaxations of the underlying crystal structure [27]. We did not account for such structural deformations in our CPA calculations but investigated their impact on the magnetic interaction using a supercell approach, and found only minor changes of the exchange constant values. Therefore, the discussion below reports results from CPA calculations.

We performed extensive Green's function calculations of $\text{Bi}_{2-x}\text{TM}_x\text{Se}_3$, $\text{Bi}_{2-x}\text{TM}_x\text{Te}_3$, and $\text{Sb}_{2-x}\text{TM}_x\text{Te}_3$ (TM = Ti, V, Cr, Mn, Fe, Co, Ni) for the range of concentrations $0 < x < 1.0$. The electronic structures of these compounds calculated within the CPA agree for low and medium concentrations ($x < 0.3$) with those of previous supercell calculations by Larson and Lambrecht [27] (see the Supplementary Material). The self-consistently obtained Green's function was further used to calculate the magnetic exchange constants J_{ij} . Their relevant directions are depicted in Fig. 1 on top of the lattice structure of $\text{Sb}_{2-x}\text{TM}_x\text{Te}_3$ for clarity, where we distinguish among in-plane (within the Sb or Bi plane) and an out-of-plane coupling. Although experimental data are available for a large concentration range [15, 16], we first focus discussion on a representative value of $x = 0.2$. The results presented in Fig. 2 can be summarized as follows.

(i) The effective exchange interaction is reduced with increasing number of d electrons per TM, going from positive to negative values. The strongest ferromagnetic interaction is found between Ti atoms, which is explained by the local density of states (DOS) of the impurities (shown in the Supplementary Material). The d electrons of Ti atoms in the majority spin channel hybridize strongly with sp states of the host. The corresponding DOS shows a strong dispersion (see the Supplementary Material) and is located mostly around the Fermi level with one occupied d orbital, while the d bonds in the minority spin channel are all unoccupied. Thus, the net

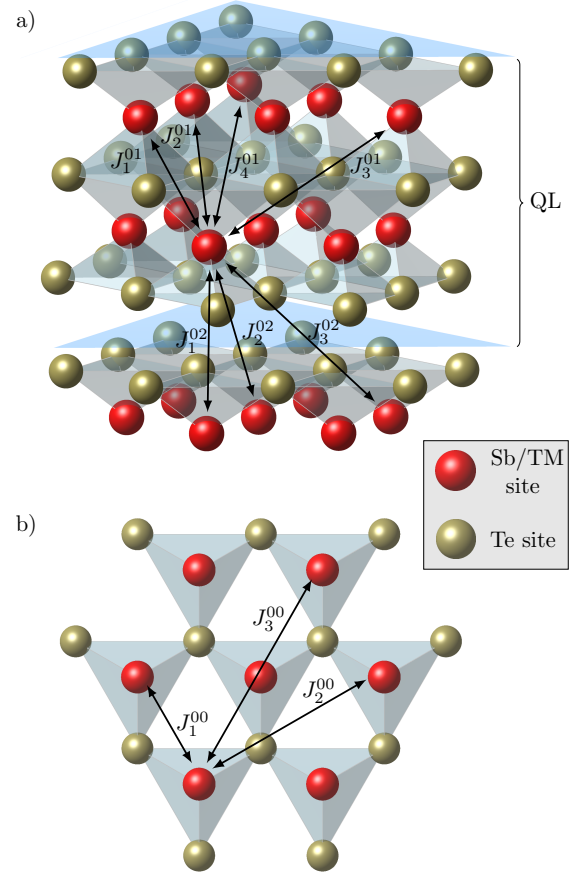


FIG. 1: (Color online) Schematic view of magnetic interactions in magnetic $\text{Sb}_{2-x}\text{TM}_x\text{Te}_3$: exchange interactions between different layers (a) and within a single layer (b), respectively. The corresponding exchange constants for Ti, V, Cr, Mn, Fe, and Co are shown in Fig. 2. The same plot applies to $\text{Bi}_{2-x}\text{TM}_x\text{Te}_3$ and $\text{Bi}_{2-x}\text{TM}_x\text{Se}_3$.

magnetization is $1.0 \mu_B/\text{atom}$, indicating a valency of 3+ for each Ti atom. The strongly dispersed DOS at the Fermi energy leads to a large ferromagnetic coupling between the nearest magnetic moments within the Sb plane (Fig. 2).

(ii) With increasing number of d electrons per TM atom, the spectral weight at the Fermi level is reduced. This leads to a strong decrease of the exchange interactions in $\text{Sb}_{2-x}\text{Mn}_x\text{Te}_3$, in which the majority and minority spin d electrons are well separated in energy and show minor dispersion. In the case of Fe impurities, due to an occupied minority spin d state at the Fermi level, the magnitude of the exchange interaction increases but becomes negative because of the large exchange splitting and the isolated impurity-like character of the occupied d orbitals. For Co and Ni impurities, the valency changes from 3+ to 2+ and 1+, respectively, reducing, thereby, the magnitude of the exchange interaction, which remains negative. The exchange interaction of $\text{Sb}_{2-x}\text{Ni}_x\text{Te}_3$, $\text{Bi}_{2-x}\text{Ni}_x\text{Te}_3$, and $\text{Bi}_{2-x}\text{Ni}_x\text{Se}_3$ is very

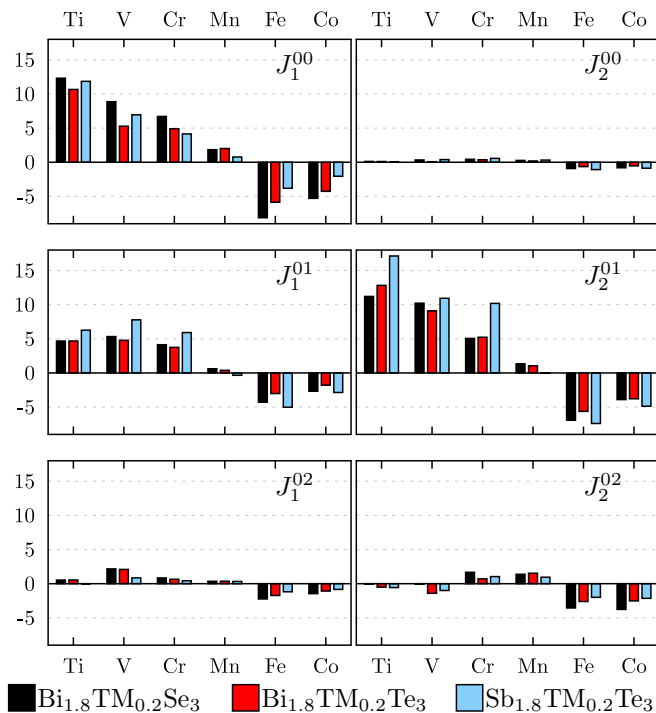


FIG. 2: (Color online) Exchange constants (in meV) in magnetic $\text{Bi}_{1.8}\text{TM}_{0.20}\text{Se}_3$, $\text{Bi}_{1.8}\text{TM}_{0.20}\text{Te}_3$, and $\text{Sb}_{1.8}\text{TM}_{0.20}\text{Te}_3$ (TM = Ti, V, Cr, Mn, Fe, Co). See the schematic view of magnetic interactions in Fig. 1.

weak and is not discussed here.

(iii) For almost all cases, the strongest exchange interaction is found between magnetic moments located in different Sb (Bi) planes but within the same quintuple layer (panel J_2^{01} in Figs. 1 and 2). The coupling weakens systematically with the number of d electrons. This interaction occurs via a Te (Se) atom lying between two impurities and is of double exchange type. In addition, the magnitude of J_1^{01} is as large as for the in-plane interaction between the nearest magnetic moments, which is an indirect exchange interaction mediated by free carrier sp states [36]. We thus conclude that two different exchange mechanisms, the double exchange interaction via an anion and the indirect exchange coupling via free carriers, determine the magnetic order in the TM doped chalcogenides.

(iv) The size of cation atoms is crucial for the exchange interaction. The large size of atoms and, thus, the more spatially extended wave functions, can lead to a strong hybridization with the electronic states of the neighboring atoms. On the one hand, this can increase the number of free carriers within the cation layer, favoring the indirect exchange of Zener type [36]. On the other hand, the strong binding between a cation (e.g. Bi) and an anion (e.g. Te) reduces the number of valence electrons of the anion and, thereby, reduces the strength of the double ex-

change interaction. Therefore, in the case of Sb_2Te_3 , the double exchange interaction via Te atoms is significantly larger than that in Bi_2Te_3 and Bi_2Se_3 .

(v) Surprisingly the exchange interaction between magnetic moments located in neighboring quintuple layers does not vanish (see J_1^{02} and J_2^{02} in Figs. 1 and 2). The spin density $m(z) \equiv [\rho_\uparrow(z) - \rho_\downarrow(z)]/[\rho_\uparrow(z) + \rho_\downarrow(z)]$ (where $\rho_\uparrow(z)$ and $\rho_\downarrow(z)$ stand for the spin-up and -down charge densities, respectively, integrated over the lateral coordinates x and y) “bridges” the van der Waals gap and is responsible for the “interquintuple layer” magnetic interaction (Fig. 3). The spin density in anion layers is negative and has a magnitude comparable with that of the spin density in the van der Waals gap.

Considering a wider range of concentrations of the TM atom, we have estimated the critical temperatures T_C using a Monte Carlo method [37–39]. To treat both ferromagnetic and antiferromagnetic materials, we investigate the spin-spin-correlation function

$$S = \sum_i \sum_{j \in \Omega_i} |\vec{m}_i \cdot \vec{m}_j|,$$

where \vec{m}_i and Ω_i are the magnetic moment and the interaction sphere around site i , respectively. We also account for percolation effects, using pair potentials, and compared estimated critical temperatures with the available experimental data. The results for ferromagnetic $\text{Sb}_{2-x}\text{TM}_x\text{Te}_3$ (TM = Ti, V, Cr, Mn; Fig. 4) show a systematic increase of the T_C with the concentration of dopants. Percolation effects do not affect strongly the behavior of T_C at low concentrations; except in the case of Ti, for which percolation lowers T_C . Calculations for Cr reproduce the experimentally measured trends for concentrations up to $x = 0.6$ [16]. For higher concentrations, we found a transition to antiferromagnetic order (area with a light red background in Fig. 4), which is understood as the results of an increasing antiferromagnetic interaction between magnetic moments from nearby quintuple layers. This explains why experimental data is unavailable for concentrations larger than $x = 0.6$.

Concerning the $\text{Sb}_{2-x}\text{V}_x\text{Te}_3$ case, we reproduce the trend found in experiments for a broad concentration range [15]. However, the theoretical absolute values are underestimated by about a factor of 1/2. One could speculate that either structural imperfections due to sample preparations or limitations in the *ab initio* description could cause this mismatch. For the reported cases of Mn doping at low concentration regimes ($x \leq 0.1$), our calculations are, again, in qualitative agreement with experiment [10, 14, 19, 40–42].

The systematic study of exchange interaction discussed for TM-doped magnetic chalcogenides elucidated in this Letter can open new possibilities for a specific design of their magnetic properties. We infer for instance that one way to control the magnetic interaction and the Curie temperature is to replace particular atoms or sheets of

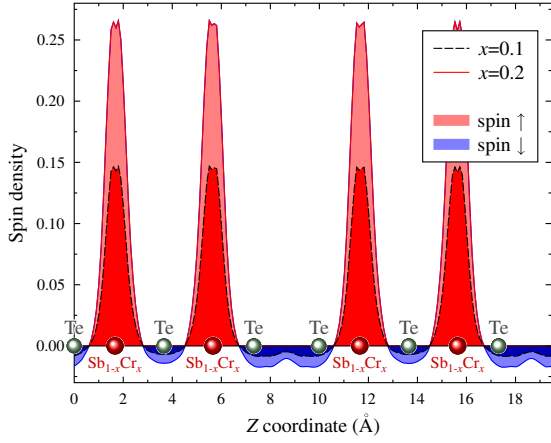


FIG. 3: (color online) Spin density $m(z)$ (see the text) of $\text{Sb}_{2-x}\text{Cr}_x\text{Te}_3$ for $x = 0.1$ and $x = 0.2$ in the $[0001]$ direction integrated over all in-plane coordinates x and y . The z range covers two quintuple layers.

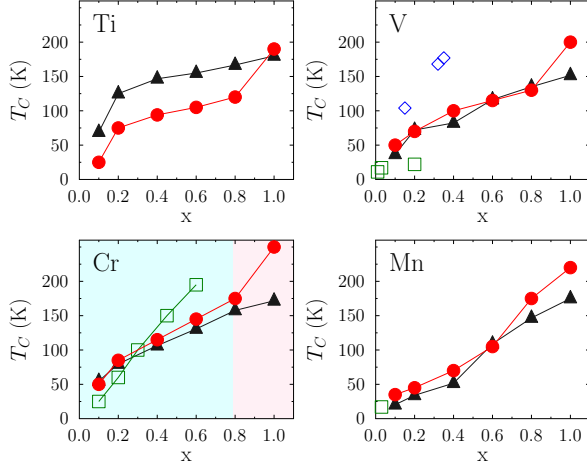


FIG. 4: (color online) Calculated critical temperature T_C versus concentration x of Ti, V, Cr, and Mn in $\text{Sb}_{2-x}\text{TM}_x\text{Te}_3$. The critical temperature T_C is determined from Monte Carlo simulations with randomly distributed impurities (black filled triangles) and with cluster percolation (red filled circles). T_C is compared to experimental data (green and blue markers) [15, 16]. In the case of Cr, there is a transition from a ferromagnetic state for $x < 0.8$ (light blue background) to an antiferromagnetic state at higher concentrations (light red background).

atoms, in order to tune the strength of the electronic hybridization; the latter is responsible for the exchange interaction mechanisms in this class of materials. Here, it has been shown that the overlap between electronic wave functions of anions and cations is crucial.

In an experimental realization, one could replace the anion layer between two cation sheets by atoms of the same group in the periodic table. As an example, we consider the layer between two $\text{Sb}_{1.80}\text{Cr}_{0.20}$ sheets in the

$\text{Sb}_{1.80}\text{Cr}_{0.20}\text{Te}_3$ alternated with various chalcogen atoms. We observe an increase of the associated Curie temperature with ionic size and spatial extension of the electronic wave function of the chalcogen ion: S, Se, Te, and Po yield $T_C = 69$ K, 71 K, 76 K, and 79 K, respectively. A similar effect can be achieved with specific co-doping of the corresponding anion layer.

The in-plane exchange interaction can instead be tuned by co-doping of the cation layers in accordance with the exchange constant behavior presented in Fig. 2. To illustrate this aspect, we calculated the exchange interaction in $\text{Bi}_{2-x-y}\text{Cr}_x\text{Sb}_y\text{Te}_3$ for $x = 0.2$ and $y = 0.0, 0.2$, and 0.4 (detailed results are presented in the Supplementary Material). Here, the Curie temperature increases with Sb concentration from 35 K at $y = 0.0$ to 39 K at $y = 0.2$, and to 42 K at $y = 0.4$.

Another way to tune the magnetic interaction is to insert impurities into the van der Waals gap [43]. This can change the size of the van der Waals gap and, by a proper choice of the impurities, can supply free carriers, which are important for the indirect exchange of Zener type (see the Supplementary Material).

In summary, we have studied the exchange interaction in the Bi_2Te_3 , Bi_2Se_3 , and Sb_2Te_3 tetradymite chalcogenides doped with transition metals. Our first principles calculations have shown that the magnetic interaction is long-range and is mainly mediated out-of-plane by the double exchange mechanism via an anion and in-plane by the indirect exchange coupling via free carriers. The calculated Curie temperatures as a function of the concentration are found in qualitative agreement with available experimental data. Finally, we presented several ways to tune the magnetic interaction in these systems: (i) replacing the anion layer between two cation sheets by atoms of the same group, (ii) co-doping of the cation sheet, and (iii) inserting impurities in the van der Waals gap. These results provide deep insight into the magnetic interactions in the magnetic binary chalcogenides, and open new ways to design new materials for promising applications.

We acknowledge support by the Ministry of Education and Science of Russian Federation (state task No. 2.8575.2013) and the Deutsche Forschungsgemeinschaft (Priority Program SPP 1666 "Topological Insulators"). The calculations were performed at the Rechenzentrum Garching of the Max Planck Society (Germany) and at the SKIF-Cyberia supercomputer of Tomsk State University.

* Electronic address: mgarcia@mpi-halle.de

† Electronic address: aernst@mpi-halle.de

[1] G. Nolas, J. Sharp, and J. Goldsmid, *Thermoelectrics: Basic Principles and New Materials Developments*, Springer Series in Materials Science (Springer, 2001).

- [2] M. Z. Hasan and C. L. Kane, *Rev. Mod. Phys.* **82**, 3045 (2010).
- [3] X.-L. Qi and S.-C. Zhang, *Rev. Mod. Phys.* **83**, 1057 (2011).
- [4] S. V. Eremeev, G. Landolt, T. V. Menshchikova, B. Slomski, Y. M. Koroteev, Z. S. Aliev, M. B. Babanly, J. Henk, A. Ernst, L. Patthey, et al., *Nat Commun* **3**, 635 (2012).
- [5] I. Žutić, J. Fabian, and S. Das Sarma, *Rev. Mod. Phys.* **76**, 323 (2004).
- [6] K. Sato, L. Bergqvist, J. Kudrnovský, P. H. Dederichs, O. Eriksson, I. Turek, B. Sanyal, G. Bouzerar, H. Katayama-Yoshida, V. A. Dinh, et al., *Rev. Mod. Phys.* **82**, 1633 (2010).
- [7] K. Uchida, S. Takahashi, K. Harii, J. Ieda, W. Koshibae, K. Ando, S. Maekawa, and E. Saitoh, *Nature* **455**, 778 (2008).
- [8] G. E. W. Bauer, E. Saitoh, and B. J. van Wees, *Nat Mater* **11**, 391 (2012).
- [9] J. S. Dyck, P. Hajek, P. Lostak, and C. Uher, *Phys. Rev. B* **65**, 115212 (2002).
- [10] J. S. Dyck, P. Svanda, P. Lostak, J. Horak, W. Chen, and C. Uher, *Journal of Applied Physics* **94**, 7631 (2003).
- [11] J. S. Dyck, C. Drasar, P. Lostak, and C. Uher, *Phys. Rev. B* **71**, 115214 (2005).
- [12] V. A. Kulbachinskii, A. Y. Kaminsky, K. Kindo, Y. Narumi, K.-i. Suga, P. Lostak, and P. Svanda, *Physica B: Condensed Matter* **329-333**, Part 2, 1251 (2003).
- [13] V. Kulbachinskii, P. Tarasov, and E. Brück, *Journal of Experimental and Theoretical Physics* **101**, 528 (2005).
- [14] J. Choi, S. Choi, J. Choi, Y. Park, H.-M. Park, H.-W. Lee, B.-C. Woo, and S. Cho, *Phys. Stat. Sol. (b)* **241**, 1541 (2004).
- [15] Z. Zhou, Y.-J. Chien, and C. Uher, *Applied Physics Letters* **87**, 112503 (2005).
- [16] Z. Zhou, Y.-J. Chien, and C. Uher, *Phys. Rev. B* **74**, 224418 (2006).
- [17] Z. Zhou, M. Zabeik, P. Lostak, and C. Uher, *Journal of Applied Physics* **99**, 043901 (2006).
- [18] J. W. G. Bos, M. Lee, E. Morosan, H. W. Zandbergen, W. L. Lee, N. P. Ong, and R. J. Cava, *Phys. Rev. B* **74**, 184429 (2006).
- [19] Y. S. Hor, P. Roushan, H. Beidenkopf, J. Seo, D. Qu, J. G. Checkelsky, L. A. Wray, D. Hsieh, Y. Xia, S.-Y. Xu, et al., *Phys. Rev. B* **81**, 195203 (2010).
- [20] D. Hsieh, Y. Xia, D. Qian, L. Wray, F. Meier, J. H. Dil, J. Osterwalder, L. Patthey, A. V. Fedorov, H. Lin, et al., *Phys. Rev. Lett.* **103**, 146401 (2009).
- [21] J. Honolka, A. A. Khajetoorians, V. Sessi, T. O. Wehling, S. Stepanow, J.-L. Mi, B. B. Iversen, T. Schlenk, J. Wiebe, N. B. Brookes, et al., *Phys. Rev. Lett.* **108**, 256811 (2012).
- [22] L. R. Shelford, T. Hesjedal, L. Collins-McIntyre, S. S. Dhesi, F. Maccheronzi, and G. van der Laan, *Phys. Rev. B* **86**, 081304 (2012).
- [23] D. West, Y. Y. Sun, S. B. Zhang, T. Zhang, X. Ma, P. Cheng, Y. Y. Zhang, X. Chen, J. F. Jia, and Q. K. Xue, *Phys. Rev. B* **85**, 081305 (2012).
- [24] M. R. Scholz, J. Sánchez-Barriga, D. Marchenko, A. Varykhalov, A. Volykhov, L. V. Yashina, and O. Rader, *Phys. Rev. Lett.* **108**, 256810 (2012).
- [25] X. F. Kou, W. J. Jiang, M. R. Lang, F. X. Xiu, L. He, Y. Wang, Y. Wang, X. X. Yu, A. V. Fedorov, P. Zhang, et al., *Journal of Applied Physics* **112**, 063912 (2012).
- [26] M. Ye, S. V. Eremeev, K. Kuroda, E. E. Krasovskii, E. V. Chulkov, Y. Takeda, Y. Saitoh, K. Okamoto, S. Y. Zhu, K. Miyamoto, et al., *Phys. Rev. B* **85**, 205317 (2012).
- [27] P. Larson and W. R. L. Lambrecht, *Phys. Rev. B* **78**, 195207 (2008).
- [28] R. Yu, W. Zhang, H.-J. Zhang, S.-C. Zhang, X. Dai, and Z. Fang, *Science* **329**, 61 (2010).
- [29] J.-M. Zhang, W. Zhu, Y. Zhang, D. Xiao, and Y. Yao, *Phys. Rev. Lett.* **109**, 266405 (2012).
- [30] J. Henk, A. Ernst, S. V. Eremeev, E. V. Chulkov, I. V. Maznichenko, and I. Mertig, *Phys. Rev. Lett.* **108**, 206801 (2012).
- [31] J. Henk, M. Flieger, I. V. Maznichenko, I. Mertig, A. Ernst, S. V. Eremeev, and E. V. Chulkov, *Phys. Rev. Lett.* **109**, 076801 (2012).
- [32] J. P. Perdew and Y. Wang, *Phys. Rev. B* **45**, 13244 (1992).
- [33] J. P. Perdew, K. Burke, and M. Ernzerhof, *Phys. Rev. Lett.* **77**, 3865 (1996).
- [34] B. L. Gyorffy, *Phys. Rev. B* **5**, 2382 (1972).
- [35] A. I. Liechtenstein, M. I. Katsnelson, V. P. Antropov, and V. A. Gubanov, *Journal of Magnetism and Magnetic Materials* **67**, 65 (1987).
- [36] C. Zener, *Phys. Rev.* **81**, 440 (1951).
- [37] N. Metropolis, A. W. Rosenbluth, M. N. Rosenbluth, and E. Teller, *J. Chem. Phys.* **21**, 1087 (1953).
- [38] K. Binder, *Rep. Prog. Phys.* **60**, 487 (1997).
- [39] G. Fischer, M. Dane, A. Ernst, P. Bruno, M. Lueders, Z. Szotek, W. Temmerman, and W. Hergert, *Physical Review B (Condensed Matter and Materials Physics)* **80**, 014408 (2009).
- [40] J. Choi, H.-W. Lee, B.-S. Kim, S. Choi, J. Choi, J. H. Song, and S. Cho, *Journal of Applied Physics* **97**, 10D324 (2005).
- [41] J. Choi, H.-W. Lee, B.-S. Kim, H. Park, S. Choi, S. Hong, and S. Cho, *Journal of Magnetism and Magnetic Materials* **304**, e164 (2006).
- [42] Y. H. Choi, N. H. Jo, K. J. Lee, H. W. Lee, Y. H. Jo, J. Kajino, T. Takabatake, K.-T. Ko, J.-H. Park, and M. H. Jung, *Applied Physics Letters* **101**, 152103 (2012).
- [43] M. M. Otrokov, S. D. Borisova, V. Chis, M. G. Vergniory, S. V. Eremeev, V. M. Kuznetsov, and E. V. Chulkov, *JETP Letters* **96**, 714 (2013).